OPTICAL REVIEW Vol. 20, No. 5 (2013) 361–366

Self-Assembled Ag Nanoparticles for Surface Enhanced Raman Scattering

Shuangmei ZHU[1,2], Chunzhen FAN[1,3], Junqiao WANG[1], Jinna HE[1], and Erjun LIANG[1]*

[1]*School of Physical Science and Engineering and Key Laboratory of Materials Physics of Ministry of Education of China, Zhengzhou University, Zhengzhou 450052, China*
[2]*Department of Mathematical and Physical Sciences, Henan Institute of Engineering, Zhengzhou 451191, China*
[3]*State Key Laboratory of Surface Physics and Department of Physics, Fudan University, Shanghai 200433, China*

(Received February 27, 2013; Accepted June 26, 2013)

Uniform and reproducible substrates for surface enhanced Raman scattering (SERS) are fabricated by self-assembly of Ag nanoparticles (NPs) on 3-aminopropyltrimethoxysilane (APTES) modified glass. Experimental results indicate that the Ag NPs with a narrow size distribution were assembled as a sub-monolayer which exhibits an excellent SERS-activity. The SERS enhancement factor is estimated to be 7.5×10^6 and the detection limit for crystal violet (CV) solution is about $\sim 10^{-11}$ M. The uniformity and reproducibility of the SERS signals are tested by point-to-point and batch-to-batch measurements. It is confirmed that the self-assembled Ag NPs substrates has a high SERS reproducibility and a low standard deviation with respect to the Ag NPs on non-functionalized glass substrates. The self-assembled Ag NPs substrates can be widely used for the application of chemical and biochemical sensing.

Keywords: Ag nanoparticles, self-assembled substrate, surface enhanced Raman scattering

1. Introduction

Raman spectroscopy is a useful technique in surface analysis, which can provide precise information on the vibrational energies of molecules to determine their detailed structural information.[1,2] However, an intrinsically small Raman scattering cross section limits its practical applications. In 1974, Fleischmann et al.[3] reported the first high-quality Raman spectra of monolayer-adsorbed pyridine on an electrochemically roughened Ag electrode surface, which was later called as surface enhanced Raman scattering (SERS). SERS is an unusual optical effect based on a nanoscale rough surface, particles or their aggregations, which can detect monolayer or sub-monolayer molecule and investigate molecular structure.[4] The discovery of SERS has aroused great interest in various fields, including physics science (search for the hot spots and exploration of the enhanced mechanism of SERS), chemistry (single-molecule detection and trace analysis of metal cations), and life science (early detection and monitoring of diseases or treatment of living cells),[5–10] which are implemented on the dramatic increase in Raman signals from molecules that have been adsorbed onto or in the vicinity of nanometer-sized metallic particles or films.[11] Theoretically, two mechanisms are playing leading roles in the explanations of SERS enhancements, namely, a long-range electromagnetic enhancement theory and a short-range chemical enhancement theory.[5] The electromagnetic enhancement results from an interaction of the incident laser radiation with electrons on the metal surface or collective oscillations of the metal electrons, while the chemical enhancement reflects the chemical interaction between the adsorbate and the metal surface. It has been generally accepted that SERS is dominated by strong electromagnetic field enhancement near metallic nanostructures, where surface plasmon coupling at the junctions or gaps between these structures creates hot spots. The coupling effects are responsible for the enormous enhancement necessary for high sensitivity of SERS detection.[12–14]

One critical aspect of SERS substrates for practical applications depends on its SERS activity, uniformity and good reproducibility.[15] The activity of SERS substrate refers to high SERS sensitivity; high uniformity stands for the deviation in enhancement over the whole surface being less than 20% and a good reproducibility indicates the deviation in the enhancement should be less than 20% for different batches of substrates prepared by the same method. To fabricate an ideal SERS substrate, electron beam lithography, nanoimprint lithography, Langmuir–Blodgett method, template method and self-assembly method have been widely employed.[16–20] Among these methods, Langmuir–Blodgett method, template method, electron beam lithography and nanoimprint lithography can produce ordered and uniform nanostructures with various shapes and geometries, but such techniques need costly instruments and harsh experiment conditions, which presents a barrier to future mass production. Alternately, with self-assembly method, simple, settable, mass-producible, inexpensive SERS substrates can circumvent these issues and offer the potential for future large-scale applications.[21,22]

Resort to the self-assembled strategy, one moiety of a bifunctional molecule, such as APTES, could anchor to the solid support through a surface polymerization procedure or displacement reaction, leaving another moiety "free" to immobilize nanomaterials from a colloid/solution via electrostatic or covalent interactions. This approach has been demonstrated to be feasible not only for electrochemical and surface plasmon resonance (SPR) sensors,[23,24] but

*E-mail address: ejliang@zzu.edu.cn

also for SERS substrates.[25,26] Freeman et al.[20] was the first to report the self-assembled metal colloid monolayers on polymer-coated substrates for SERS. Particles were bound to the substrate through multiple bonds between the colloidal metal and functional groups on the polymer APTES. Recently, Moskovits and Jeong[27] also reported that Au NPs monolayers assembled on quartz slides modified by amine moieties. Zhai et al.[28] reported a multiple deposition approach of Ag NPs on chemically modified agarose films and revealed a maximum SERS intensity with four layers of the Ag NPs deposition. Spiked gold beads self-assembled into thin films on APTES modified glass was also exploited for single particle SERS.[29]

In this paper, we primarily focus on the fabrication of monolayer silver films on the surfaces of glass slides to achieve uniform and reproducible SERS substrates with electrostatic self-assembled Ag NPs. The characterizations of the monolayer substrates were carried out by scanning electron microscopy (SEM) and UV–vis absorption method. The activity, uniformity and reproducibility of the substrates for SERS are tested by using crystal violet (CV) as the probe molecule. It is shown that the self-assembled SERS substrates are uniform in NPs size and distribution, and have high reproducibility, uniformity and activity for SERS applications.

2. Experimental Procedure

2.1 *Materials and instruments*

Silver nitrate ($AgNO_3$), sodium citrate ($Na_3C_6H_5O_7 \cdot H_2O$), sulfuric acid (H_2SO_4), hydrogen peroxide (H_2O_2), ammonia water ($NH_3 \cdot H_2O$), and crystal violet (CV) were purchased from Zhengzhou Fuyou Chemical (China). 3-Aminopropyltriethoxysilane (APTES, 97%) was purchased from Beijing Chemical (China). All chemical reagents were used as purchased without further processing. Aqueous solutions were prepared using distilled de-ionized water.

Characterizations of the self-assembled Ag NPs films were performed by a JEOL JSM-6700F field emission scanning electron microscopy (FE-SEM). UV–vis absorption spectra of Ag NPs were taken by using a Shimadzu UV 3150 UV–vis–NIR spectrophotometer. Surface enhanced Raman scattering was detected by a Renishaw 2000 Raman spectrometer with 532 nm laser excitation. The laser was focused onto the samples from the top by a 50× objective (NA = 0.55), and the reflected Raman signals are collected through the same objective. The diameter of laser spot and penetration depth of the focused laser beams are ~0.59 and ~18 μm, respectively.

To detect the Raman spectra of the CV molecule, 20 μL of CV solution with different concentrations was dropped onto the surfaces of the self-assembled Ag substrates. SERS spectra of CV molecule on the self-assembled Ag substrates were recorded after the evaporation of CV solution.

2.2 *Preparation of SERS-active substrates*

Synthesis of Ag NPs:[30] 18 mg silver nitrate was dissolved in 150 mL de-ionized water at 70 °C and then the aqueous solution was rapidly heated to boiling point. After that 1% solution of sodium citrate (2 mL) was added rapidly under vigorous stirring. The solution was kept at boiling point for 1 h, and then cooled down to room temperature with constant stirring. Finally, the solution was employed for UV–vis study and SEM analysis.

Cleaning, activation and silanization of the glass substrates: all glass slips were washed sequentially with de-ionized water, acetone, ethanol and de-ionized water for at least 20 min in an ultrasonic bath, respectively. The cleaned glass slides were quickly immerged in piranha solution ($H_2O_2/H_2SO_4 = 3:7$, v/v), boiled for 30 min at 80 °C, and then washed with de-ionized water. They were transferred apace in mixed solution of $H_2O_2/NH_3/H_2O$ (1 : 1 : 5, v/v/v) and boiled for another 30 min at 75 °C, and then washed with de-ionized water. Finally, the surface-activated glass slips were vertically immersed rapidly in a 1% (v/v) solution of APTES in anhydrous ethanol for 24 h. After that, the substrates were rinsed thoroughly (at least three times) in ethanol to remove excess silane coupling reagent, and dried at 110 °C in an air oven for 1 h.

Self-assembled Ag NPs: The silanized slips were vertically dipped into the Ag NPs solution for 12 h to prepare the self-assembled substrates. Finally, these substrates were washed with de-ionized water for further use. The size of all squared self-assembled Ag substrates is the same, which is 0.5 cm^2.

Self-assembled Ag NPs on a blank glass slip (non-functionalized glass substrates): the glass slips were washed sequentially with de-ionized water, acetone, ethanol and de-ionized water for at least 20 min in an ultrasonic bath, respectively. After that, 20 μL of Ag sols was dropped onto the surfaces of glass with a square 0.5 cm^2. Then, the substrates dried at in air for further use.

3. Results and Discussion

3.1 *Schematic process of the self-assembled substrates*

Schematic procedures to prepare the self-assembled substrates are demonstrated in Fig. 1. After cleaning of the glass substrates in the mixed solution as shown in Fig. 1(a), they were dipped into the APTES solution, where the ethoxy groups of APTES were easily hydrolyzed into Si–OH, then interacts with the Si–OH of glass surface to form hydrogen bond. After washing out the non-hydrogen bond of APTES on the glass surface, silanol groups would be dehydrated to form Si–O–Si bond through heating treatment.[31] Finally, a film with terminal amino-group was formed as shown in Fig. 1(c). The surface of the silanized glass is positively charged, which favors the negative-charged silver NPs to adsorb through electrostatic interaction. In order to form a uniform substrate, the capping agents APTES were used to prevent the aggregation of Ag NPs. During the self-assembly process, stirring was necessary to increase the homogeneity of the substrates. It is believed that the derivitization process causes a silane layer to bond to –OH functional groups on the surface. As a result, APTES-functionalized self-assembly of Ag NPs on glass slides is realized.

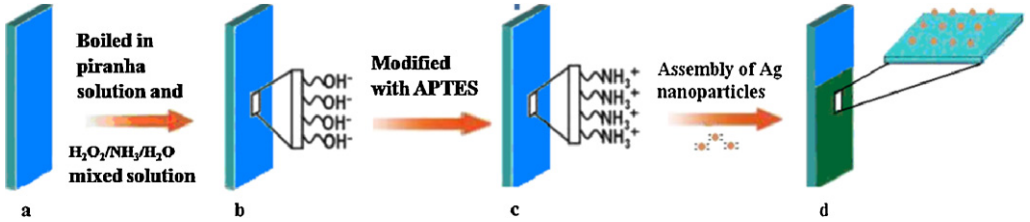

Fig. 1. (Color online) Schematic processes of self-assembled Ag NPs on the APTES-functionalized glass substrates.

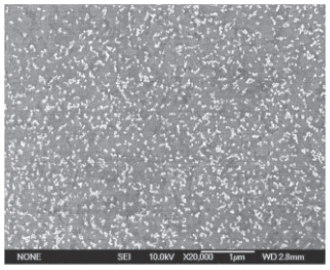

(a)

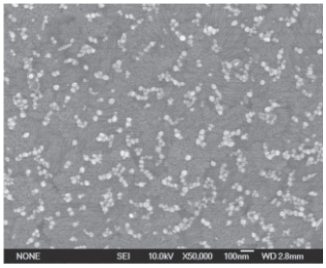

(b)

Fig. 2. SEM images of the self-assembled Ag NPs on (a) the APTES-functionalized glass substrates and (b) the nonfunctionalized glass substrates.

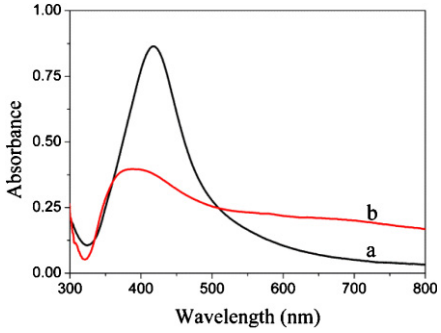

Fig. 3. (Color online) Absorption spectra of silver colloids (a) and the self-assembled Ag NPs (b).

3.2 *SEM images of the substrate and UV–vis absorption spectra*

The SEM images of APTES-functionalized substrates and non-functionalized glass substrates with self-assembled Ag NPs are illustrated in Figs. 2(a) and 2(b), respectively. The assembled Ag NPs distributed as monolayer or sub-monolayer on the APTES-functionalized glass slips as shown in Fig. 2(a). The Ag NPs with fairly uniform diameter around 50 nm are uniformly distributed on APTES-functionalized glass. However, the distribution of the Ag NPs on the non-functionalized glass is quite irregular. The Ag NPs tend to aggregate in some areas, leaving the rests of the substrate empty. Ag NPs on the non-functionalized glass cannot be expected as uniform and reproducible SERS substrate. For nanosized particles, whose dimension is much smaller than that of the incident light, its optical property is characterized by a broad, intense absorption band in the visible range. Figure 3(a) shows the absorption spectrum of the as-prepared silver colloids. It shows that the absorption band of the Ag NPs appears at ca. 417 nm. It was caused by the interaction of incident light with free electrons in the Ag NPs, which is known as surface plasmon resonance (SPR). Their bandwidth, peak height, and peak position can be effectively tuned by the size, shape, surface coverage, and surrounding environment, etc.[32] Figure 3(b) shows the UV–vis absorption spectrum of the assembled silver NPs. Compared with the silver colloid, it can be clearly observed that the resonant peak (λ_{max}) of the silver NPs assembled on the APTES-functionalized glass slide is blue-shifted from 417 to 399 nm. This may be attributed to the dipole–dipole interaction between the metal particles assembled in a two-dimensional manner.[33] Meanwhile, a new feature corresponding to a collective particle surface plasmon oscillation appears around 650 nm. It happens due to the closely packed Ag NPs as shown in Fig. 2(a).[20]

3.3 *Raman spectra with self-assembled Ag NPs substrates*

Raman spectra of the CV molecule on the self-assembled Ag NPs substrate were measured with an excitation wavelength of 532 nm. The results are shown in Fig. 4. For comparison, Raman spectra of solid CV and solution of 1.0×10^{-6} M CV on glass slide were illustrated in Figs. 4(a) and 4(b). The solid CV shows very weak signals while Raman peaks of the CV solution can hardly be seen. Nevertheless, very intense Raman signals of 1.0×10^{-6} M aqueous solution of CV on self-assembled substrate are observed, as shown in Fig. 4(c). The assignments of the Raman modes are displayed in Table 1 following the work of Liang et al.[34,35] The spectral signal from the CV bases is 339 cm^{-1} band, which is attributed to the in-plane vibration of ph–C^+–ph bending. The Raman band at 422 cm^{-1} is ascribed to the out-of-plane vibration of ph–C^+–ph bend.

Table 1. Observed wave-numbers (cm^{-1}) in normal Raman and SERS spectra of CV and their assignment (based on Refs. 34 and 35).

Normal Raman (cm^{-1})	SERS of self-assembled substrates (cm^{-1})	Vibration assignment
341	339	In-plane vibration of ph–C^+–ph bend
422	422	Out-of-plane vibration of ph–C^+–ph bend
528, 563	525, 562	Ring skeletal vibration of radical orientation
728, 770, 826	726, 760, 805	Out-of-plane vibration of ring C–H bend
920	913	Ring skeletal vibration of radical orientation
1175, 1229	1175, 1298	In-plane vibration of ring C–H bend
1539	1539	Phenyl ring C–C stretching + N^+=phenyl stretching
1583	1588	Phenyl ring C–C stretching and bend
1616	1620	Phenyl ring C–C stretching + N–phenyl stretching

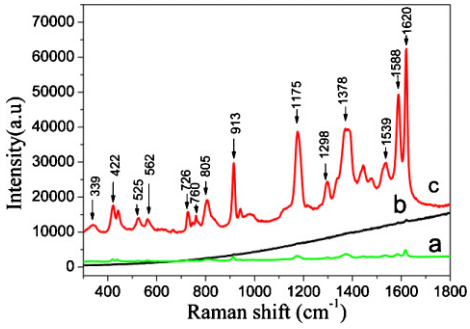

Fig. 4. (Color online) Raman spectra of solid CV (a) and 1.0×10^{-6} M (b) on glass slide. (c) SERS spectrum of 1.0×10^{-6} M aqueous solution of CV on self-assembled substrate.

The peaks at 528, 562, 913 cm^{-1} are assigned to the ring skeletal vibration of radial orientation and the peaks at 726, 760, 805, 1175 cm^{-1} are responsible for the ring (C–H) bending mode, respectively. In addition, the peaks at ca. 1298, 1539, 1588, 1620 cm^{-1} are caused by the ring C–C stretching vibration.

To quantitatively define the enhancement effect of CV on the Ag NPs self-assembled substrate, we calculated the surface enhancement factor (EF) which is defined as[36,37]

$$\mathrm{EF} = \frac{I_{\mathrm{surf}}/N_{\mathrm{surf}}}{I_{\mathrm{vol}}/N_{\mathrm{vol}}},$$

where I_{surf} is the intensity of a vibrational mode in the SERS spectrum of CV and I_{vol} stands for the intensity of the same vibration mode in the Raman spectrum of the solution or solid phase. I_{surf} and I_{vol} can be directly obtained from the experiment. The intensity of the in-plane vibration of the ring C–H bend at 1175 cm^{-1} is chosen to calculate the EF. According to Fig. 4, $I_{\mathrm{surf}}/I_{\mathrm{vol}} = 21361/787 = 27.142$. All spectra were normalized with the same acquisition time and laser power. N_{surf} is the number of molecules adsorbed on the SERS active substrate within the laser spot. This value can be got with the method proposed by Orendorff et al.:[37]

$$N_{\mathrm{surf}} = N_{\mathrm{d}} A_{\mathrm{laser}} A_{\mathrm{N}}/\sigma,$$

where N_{d} is the number density of the Ag NPs, A_{laser} is the focal spot area of the laser, A_{N} is the area of Ag NP's footprint, and σ is the surface area occupied by an adsorbed CV molecule. N_{d} and A_{N} can be obtained from Fig. 3, and A_{laser} is 1.09 μm^2 in our measurement. According to the report by Andrzej Kudelski,[38] each CV molecule occupies 4 nm^2 on full coverage of Ag NPs, which indicates that σ can be adopted as 4 nm^2 per molecule. Then the total number of surface adsorbed molecules (N_{surf}) on Ag NPs assembled on the silane modified glass within the illuminated laser spot is 8.662×10^4 $[(9 \times 1.09 \times 10^6 \times 3.14 \times 50^2)/(471 \times 471 \times 4)]$. N_{vol} is the molecule number of neat CV in the laser illuminated volume. In our experiment, the penetration depth of the focused laser beam is taken as 18 μm. The density of the solid CV is calculated as 0.83 g/cm^3. N_{vol} was calculated to be 2.403×10^{10} $[(0.83 \times 1.09 \times 10^{-12} \times 18 \times 10^{-6} \times 6.02 \times 10^{23})/10^{-6}]$ within the illuminated laser light. Therefore, the EF of our self-assembled substrates is ca. 7.5×10^6 for the in-plane ring C–H bending vibration at 1175 cm^{-1}.

To further demonstrate the advantages of the APTES-functionalized self-assembled substrate, we prepared substrates with the Ag NPs randomly positioned on a blank glass slip by doing the same procedure for comparison. SERS spectra from five random points on each substrate were measured. The results are shown in Fig. 5. The SERS spectra from point to point on our self-assembled substrate remain the same, exhibiting good uniformity as shown in Fig. 5(a). However, the SERS spectra on the non-functionalized substrate are highly position-dependent, indicating a poor uniformity as shown in Fig. 5(b). The peak height at 1175 cm^{-1} was statistically calculated for the standard deviation. For the self-assembled substrate, it has a mean value of 24922 ± 3600 counts, which is equivalent to a 14% standard deviation. The standard deviation of peak height at 1175 cm^{-1} in Fig. 5(b) is 86%, which is much larger than the functionalized substrate. Therefore, APTES-functionalized self-assembled substrates can greatly improve the uniformity as well as enhance the Raman intensity due to the uniform size and distribution of the self-assembled Ag NPs.

The batch-to-batch variation has been done with the test CV molecule to investigate the reproducibility of self-assembled Ag NPs. Five pieces of self-assembled Ag NPs

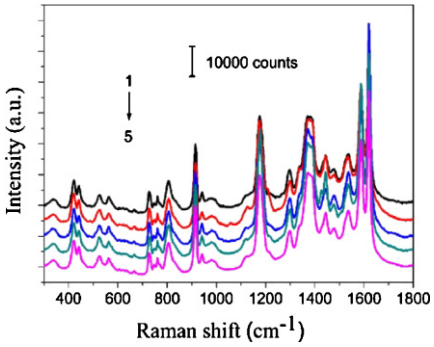

(a)

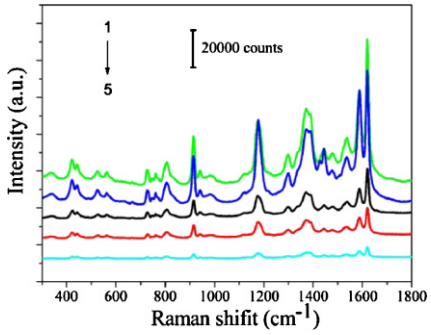

(b)

Fig. 5. (Color online) SERS spectra of 1.0×10^{-6} M CV adsorbed on the self-assembled substrate (a) and blank substrate (b). Five random points were measured.

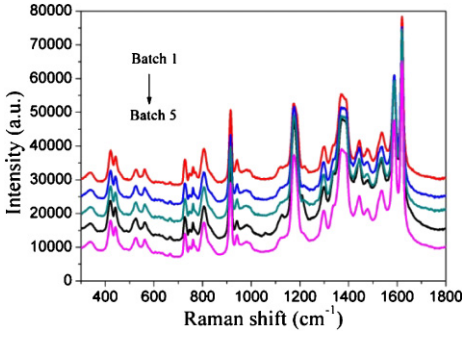

(a)

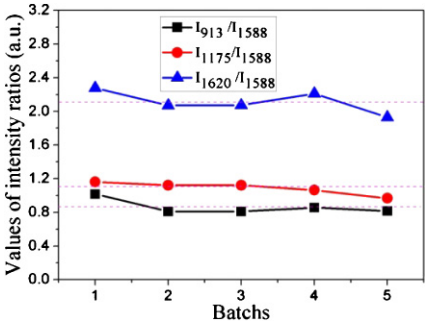

(b)

Fig. 6. (Color online) (a) SERS spectra of 10^{-6} M CV molecules adsorbed on five different self-assembled Ag substrates. (b) Average relative intensity of Raman bands at 913/1588, 1175/1588, 1620/1588 cm^{-1} in the SERS spectra of CV molecule. Dotted lines represent average values of intensity ratios at 913/1588, 1175/1588, 1620/1588 cm^{-1}.

on the surface of transparent glass were fabricated with the same procedure. SERS spectra of 10^{-6} M CV molecules adsorbed on five different self-assembled Ag NPs were shown in Fig. 6(a). Figure 6(b) shows the average relative intensities of the Raman bands at 913/1588, 1175/1588, 1620/1588 cm^{-1} in the SERS spectra. We find that the SERS substrates of the self-assembled Ag NPs are highly reproducible as indicated by the relative intensities of the Raman bands from batch to batch.

Figure 7 shows the SERS spectra of CV with different concentrations (10^{-6}, 10^{-7}, 10^{-8}, 10^{-9}, 10^{-10}, and 10^{-11} M) adsorbed on self-assembled Ag substrates with the assembled method. It shows that the detection limit of CV solution is down to $\sim 10^{-11}$ M. Under the concentration of 10^{-11} M, the valid Raman bands to identify CV are at 1588 and 1619 cm^{-1}. Thus, the monolayer Ag NPs by the simple method of self-assembly on the glass substrate can be employed as a perfect SERS substrate for CV detection at lower concentrations.

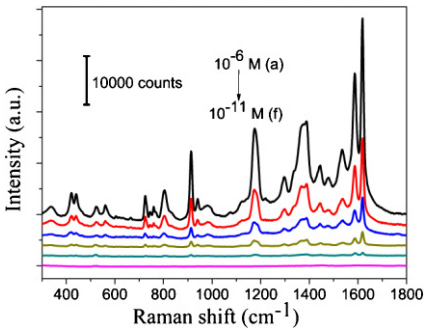

Fig. 7. (Color online) SERS spectra of CV with concentrations of 10^{-6} (a), 10^{-7} (b), 10^{-8} (c), 10^{-9} (d), 10^{-10} (e), 10^{-11} M (f) adsorbed on the self-assembled monolayers of Ag NPs.

4. Conclusions

The cost-effective SERS substrates have been prepared through the self-assembly of Ag NPs. SEM images of the substrates shows a uniform sub-monolayer distribution of the Ag NPs with regular size. The self-assembled substrates exhibit high SERS activity and reproducibility with very low variations from point to point and from batch to batch. The SERS enhancement factor for CV molecule on the self-assembled Ag NPs substrate is ca. 7.5×10^6 and the detection limit of CV solution is down to $\sim 10^{-11}$ M. As a high-performance SERS-active substrate, our proposed self-assembled Ag substrates are promising for a myriad of chemical and biochemical sensing applications, such as proteins, DNA, RNA, aminothiols, and metal ions, based on the sensing mechanism of a long-range electromagnetic enhancement theory and a short-range chemical enhancement theory.[10,39–41]

Acknowledgments

This work was supported by the National Science Foundation of China (Grant Nos. 10974183, 11104252) and by the Ministry of Education of China (Grant No. 20114101110003) and by the fund for Science and Technology innovation team of Zhengzhou (2011-03) and by the Science and Technology Program of Henan Province (Grant Nos. 112102310543, 122300410162) and the Natural Science Foundation of Henan Educational Committee (Grant No. 12A140002), by the cooperation fund with Fudan University (No. KL2011-01).

References

1) S. W. Joo, S. W. Han, and K. Kim: J. Colloid Interface Sci. **240** (2001) 391.
2) H. J. Chen, Y. L. Wang, J. Y. Qu, and S. J. Dong: J. Raman Spectrosc. **38** (2007) 1444.
3) M. Fleischmann, P. J. Hendra, and A. J. McQuillan: Chem. Phys. Lett. **26** (1974) 163.
4) Z.-Q. Tian, B. Ren, and D.-Y. Wu: J. Phys. Chem. B **106** (2002) 9463.
5) S. Nie and S. R. Emory: Science **275** (1997) 1102.
6) L. D. Qin, S. L. Zou, C. Xue, A. Atkinson, G. C. Schatz, and C. A. Mirkin: Proc. Natl. Acad. Sci. U.S.A. **103** (2006) 13300.
7) A. Kudelski: Talanta **76** (2008) 1.
8) S. J. Lee, A. R. Morrill, and M. Moskovits: J. Am. Chem. Soc. **128** (2006) 2200.
9) Y. J. Sun, L. L. Sun, B. H. Zhang, F. Xu, Z. L. Liu, C. L. Guo, Y. Zhang, and Z. Li: Talanta **79** (2009) 562.
10) J. Kneipp, H. Kneipp, M. McLaughlin, D. Brown, and K. Kneipp: Nano Lett. **6** (2006) 2225.
11) J. F. Li, Y. F. Huang, Y. Ding, Z. L. Yang, S. B. Li, X. S. Zhou, F. R. Fan, W. Zhang, Z. Y. Zhou, D. Y. Wu, B. Ren, Z. L. Wang, and Z. Q. Tian: Nature **464** (2010) 392.
12) P. G. Etchegoin, E. C. Le Ru, and M. Meyer: J. Am. Chem. Soc. **131** (2009) 2713.
13) Y. Fang, N.-H. Seong, and D. D. Dlott: Science **321** (2008) 388.
14) M. Rycenga, X. H. Xia, C. H. Moran, F. Zhou, D. Qin, Z.-Y. Li, and Y. N. Xia: Angew. Chem. **123** (2011) 5587.
15) X.-M. Lin, Y. Cui, Y.-H. Xu, B. Ren, and Z.-Q. Tian: Anal. Bioanal. Chem. **394** (2009) 1729.
16) W. S. Yue, Z. H. Wang, Y. Yang, L. Q. Chen, A. Syed, K. C. Wong, and X. B. Wang: J. Micromech. Microeng. **22** (2012) 125007.
17) S. Krishnamoorthy, S. Krishnan, P. Thoniyot, and H. Y. Low: ACS Appl. Mater. Interfaces **3** (2011) 1033.
18) N. Ahamad and A. Ianoul: J. Phys. Chem. C **115** (2011) 3587.
19) Y. Y. Li, J. Pan, P. Zhan, S. N. Zhu, N. B. Ming, Z. L. Wang, W. D. Han, X. Y. Jiang, and J. Zi: Opt. Express **18** (2010) 3546.
20) R. G. Freeman, K. C. Grabar, K. J. Allison, R. M. Bright, J. A. Davis, A. P. Guthrie, M. B. Hommer, M. A. Jackson, P. C. Smith, D. G. Walter, and M. J. Natan: Science **267** (1995) 1629.
21) V. Santhanam, J. Liu, R. Agarwal, and R. P. Andres: Langmuir **19** (2003) 7881.
22) O. S. Ivanova and F. P. Zamborini: J. Am. Chem. Soc. **132** (2010) 70.
23) S. A. Elfeky, F. D'Hooge, L. Poncel, W. Chen, S. P. Perera, J. M. H. van den Elsen, T. D. James, A. T. A. Jenkins, P. J. Cameron, and J. S. Fossey: New J. Chem. **33** (2009) 1466.
24) V. K. S. Hsiao, J. R. Waldeisen, Y. B. Zheng, P. F. Lloyd, T. J. Bunning, and T. J. Huang: J. Mater. Chem. **17** (2007) 4896.
25) K. C. Grabar, P. C. Smith, M. D. Musick, J. A. Davis, D. G. Walter, M. A. Jackson, A. P. Guthrie, and M. J. Natan: J. Am. Chem. Soc. **118** (1996) 1148.
26) M. K. Fan, G. F. S. Andrade, and A. G. Brolo: Anal. Chim. Acta **693** (2011) 7.
27) M. Moskovits and D. H. Jeong: Chem. Phys. Lett. **397** (2004) 91.
28) W.-L. Zhai, D.-W. Li, L.-L. Qu, J. S. Fossey, and Y.-T. Long: Nanoscale **4** (2012) 137.
29) P. Aldeanueva-Potel, E. Carbó-Argibay, N. Pazos-Pérez, S. Barbosa, I. Pastoriza-Santos, R. A. Alvarez-Puebla, and L. M. Liz-Marzán: ChemPhysChem **13** (2012) 2561.
30) P. C. Lee and D. Meisel: Phys. Chem. **86** (1982) 3391.
31) T. Sato, D. Brown, and B. F. G. Johnson: Chem. Commun. (1997) 1007.
32) P. Mulvaney: Langmuir **12** (1996) 788.
33) L. B. Yang, W. D. Ruan, X. Jiang, B. Zhao, W. Q. Xu, and J. R. Lombardi: J. Phys. Chem. C **113** (2009) 117.
34) E. J. Liang, X. L. Ye, and W. Kiefer: J. Phys. Chem. A **101** (1997) 7330.
35) H. R. Zhang and S. Q. Man: Chin. J. Anal. Chem. **39** (2011) 821.
36) B. Ren, X.-F. Lin, Z.-L. Yang, G.-K. Liu, R. F. Aroca, B.-W. Mao, and Z.-Q. Tian: J. Am. Chem. Soc. **125** (2003) 9598.
37) C. J. Orendorff, A. Gole, T. K. Sau, and C. J. Murphy: Anal. Chem. **77** (2005) 3261.
38) A. Kudelski: Chem. Phys. Lett. **414** (2005) 271.
39) Y. C. Cao, R. Jin, and C. A. Mirkin: Science **297** (2002) 1536.
40) R. M. Liu, M. Z. Si, Y. P. Kang, X. F. Zi, Z. Q. Liu, and D. Q. Zhang: J. Colloid Interface Sci. **343** (2010) 52.
41) R. M. Liu, S. M. Zhu, M. Z. Si, Z. Q. Liu, and D. Q. Zhang: J. Raman Spectrosc. **43** (2012) 370.